ETV6::ACSL6 translocation-driven super-enhancer activation leads to eosinophilia in acute lymphoblastic leukemia through IL-3 overexpression

Wenqian Xu,[1*] Feng Tian,[2*] Xiaolu Tai,[3] Gaoxian Song,[1] Yuanfang Liu,[1] Liquan Fan,[1] Xiangqin Weng,[1] Eunjeong Yang,[4] Meng Wang,[5] Martin Bornhäuser,[6] Chao Zhang,[3] Richard B. Lock,[7] Jason W.H. Wong,[4] Jin Wang,[1#] Duohui Jing[1#] and Jian-Qing Mi[1#]

[1]Shanghai Institute of Hematology, State Key Laboratory of Medical Genomics, National Research Center for Translational Medicine at Shanghai, Ruijin Hospital Affiliated to Shanghai Jiao Tong University School of Medicine, Shanghai, China; [2]Hebei Key Laboratory of Medical Data Science, Institute of Biomedical Informatics, School of Medicine, Hebei University of Engineering, Handan, Hebei Province, China; [3]Department of Plastic and Reconstructive Surgery, Shanghai Ninth People's Hospital, Shanghai Jiao Tong University School of Medicine, Shanghai, China; [4]School of Biomedical Sciences, University of Hong Kong, Hong Kong, China; [5]Songjiang Research Institute, Songjiang District Central Hospital, Institute of Autism & MOE-Shanghai Key Laboratory for Children's Environmental Health, Shanghai Jiao Tong University School of Medicine, Shanghai, China; [6]Medical Clinic I, University Hospital Carl Gustav Carus, TU Dresden, Dresden, Germany and [7]Children's Cancer Institute, Lowy Cancer Research Centre, School of Clinical Medicine, UNSW Medicine & Health, UNSW Centre for Childhood Cancer Research, UNSW Sydney, Sydney, New South Wales, Australia

*WX and FT contributed equally as first authors.

#JW, DJ and J-QM contributed equally as senior authors.

Correspondence: D. Jing
jdh12262@rjh.com.cn

J. Wang
jinwang@shsmu.edu.cn

J-Q. Mi
jianqingmi@shsmu.edu.cn

Received: August 22, 2023.
Accepted: February 2, 2024.
Early view: February 15, 2024.

https://doi.org/10.3324/haematol.2023.284121

Abstract

ETV6::ACSL6 represents a rare genetic aberration in hematopoietic neoplasms and is often associated with severe eosinophilia, which confers an unfavorable prognosis requiring additional anti-inflammatory treatment. However, since the translocation is unlikely to produce a fusion protein, the mechanism of *ETV6::ACSL6* action remains unclear. Here, we performed multi-omics analyses of primary leukemia cells and patient-derived xenografts from an acute lymphoblastic leukemia (ALL) patient with *ETV6::ACSL6* translocation. We identified a super-enhancer located within the *ETV6* gene locus, and revealed translocation and activation of the super-enhancer associated with the *ETV6::ACSL6* fusion. The translocated super-enhancer exhibited intense interactions with genomic regions adjacent to and distal from the breakpoint at chromosomes 5 and 12, including genes coding inflammatory factors such as *IL-3*. This led to modulations in DNA methylation, histone modifications, and chromatin structures, triggering transcription of inflammatory factors leading to eosinophilia. Furthermore, the bromodomain and extraterminal domain (BET) inhibitor synergized with standard-of-care drugs for ALL, effectively reducing *IL-3* expression and inhibiting *ETV6::ACSL6* ALL growth *in vitro* and *in vivo*. Overall, our study revealed for the first time a cis-regulatory mechanism of super-enhancer translocation in *ETV6::ACSL6* ALL, leading to an ALL-accompanying clinical syndrome. These findings may stimulate novel treatment approaches for this challenging ALL subtype.

Introduction

Chromosomal rearrangements are common in cancers, particularly hematologic malignancies.[1] In acute lymphoblastic leukemia (ALL), their characterization has led to significant improvements in risk stratification and the development of targeted therapy.[2,3] *ETV6* is reported to form fusion genes with over 30 different partners, representing one of the most frequently translocated genes in ALL.[4] While *ETV6::RUNX1*, a common *ETV6* fusion in children, indicates favorable outcomes,[4] other *ETV6* fusions indicate poor prognosis.[5,6] In addition to standard-of-care chemotherapy,

targeted therapies have been regularly applied in the clinic to inhibit the trans-regulatory activities of *ETV6* partner proteins.[5,7] Even though ETV6 is critical for hematopoiesis, its function in leukemogenesis may be underestimated compared to its partner proteins which play a dominant role in the dysregulation of downstream genes and pathways.[7,8] Moreover, the mechanisms by which various *ETV6* fusions cause malignancy remain poorly understood.

ETV6::ACSL6 t(5;12)(q31;p13) is a rare *ETV6* fusion, with only 17 cases reported in myeloid malignancies worldwide until 2022, and none in ALL. The prognosis of patients with *ETV6::ACSL6* is usually unfavorable, with most patients surviving less than a year.[9] Eosinophilia is a common complication of the disease, which often results in damage to various organs. The elevated eosinophils, in severe cases, can cause cerebral infarction and heart failure, posing life-threatening risks. This complicates the clinical care of these patients, and underscores the significance of prompt identification and treatment. Previous studies have found several pro-inflammatory mediators, including interleukin (IL)-3 and IL-5, to be up-regulated in acute myeloid leukemia (AML) with *ETV6* t(5;12) translocations.[10] While IL-5 is considered vital for the maturation and differentiation of eosinophils, IL-3 displays more potent effects on their functions.[11] However, the mechanism of IL-3 and IL-5 up-regulation in *ETV6::ACSL6* is yet to be elucidated.

Translocation events can induce trans- or cis-regulatory activities, altering gene expression profiles of cancer cells.[12] Most previous studies focused on trans-regulatory activities of oncogenic fusion proteins.[13-15] However, *ETV6::ACSL6* has been shown to be associated with frameshift mutation conferring a premature stop codon, thus unlikely to be translated into a full-length protein,[16] suggesting an alternative mechanism is involved. Cis-regulatory elements play critical roles in oncogenesis through structural variations (SV). This may cause 'regulatory rearrangements' of promoters and enhancers, leading to dysregulation of oncogenes. For example, t(8;14)(q24;q32), the most common translocation in Burkitt lymphoma, leads to *MYC* overexpression due to the relocation of an enhancer from chromosome (chr) 14 to its nearby region.[17] Furthermore, in 2004, it was shown that the ectopic expression of the homeobox gene *CDX2* resulting from the t(12;13)(p13;q12) and not the expression of the *ETV6::CDX2* fusion gene resulted in AML in a murine model.[18] Recently, *ETV6* was also demonstrated to regulate its partner gene *MN1* via super-enhancer (SE) hijacking in AML.[19] However, the mechanism is yet to be extended to other *ETV6* fusions as well as genes apart from its partners, and the clinical relevance of *ETV6*-associated SE hijacking events remains unexplored.

Coding genes of inflammatory factors, including *IL-3*, *IL-5* and *GM-CSF*, are located adjacent to *ACSL6* on chr5. This raises a question of whether and how *ETV6::ACSL6* is involved in the dysregulation of these genes. Therefore, in this study, we used multi-omics approach to interrogate the *ETV6* translocation-induced cis-regulatory mutation and changes in the 3D genome structure in *ETV6::ACSL6* ALL to decipher mechanisms of inflammatory factor dysregulation and its associated clinical syndrome eosinophilia.

Methods

Bone marrow samples from patients

Bone marrow (BM) samples from ALL patients or the healthy donor (diagnosed with thrombocytopenia, but with both BM smear and flow cytometry showing no abnormalities) were obtained under informed consent from Ruijin Hospital. Mononuclear cells were enriched by density gradient centrifugation with Ficoll solution. The use of samples was approved by the institutional review board. All relevant ethical regulations were followed in this study.

scNMT-sequencing library preparation and sequencing

scNMT-sequencing (seq) libraries were prepared according to a previous protocol.[20] Single cells were sorted using FACS Aria into 96-well plates containing 2.5 μl of reaction buffer: 1xM.CviPI buffer (NEB), 2 U M.CviPI (NEB), 160 μM S-adenosylmethionine (NEB), 1 U μl–1 RNasein (Thermo), 0.1% IGEPAL CA-630 (Sigma). After a 15-minute incubation at 37°C, RLT plus buffer (Qiagen) were added and samples stored at -80°C. Poly-A RNA was captured on oligo-dT and amplified cDNA was prepared according to Smart-seq2 protocols. The gDNA lysate was purified on AMPureXP beads before bisulfite-sequencing (BS-seq) libraries were prepared according to the scBS-seq protocol.[21] Sequencing was carried out on a NovaSeq instrument, with a mean raw sequencing depth of 7.5 million (BS-seq) and 5 million (RNA-seq) paired-end reads per cell. BS-seq alignment and methylation/accessibility quantification was performed following a previous approach.[20] Briefly, individual CpG or GpC sites of each cell were modeled using a binomial distribution, where the number of successes represented the reads supporting methylation, and the number of trials was the total read count. The CpG methylation or GpC accessibility rate for each site and cell was determined through maximum likelihood estimation. Subsequently, the rates were rounded to the nearest integer (0 or 1).

All other methods are described in detail in the *Online Supplementary Appendix*.

Results

Transcriptomic analysis of *ETV6::ACSL6* acute lymphoblastic leukemia and its accompanied eosinophils

The *ETV6::ACSL6* ALL patient is a 66-year-old male who presented to the clinic with a dry cough. The eosinophil count has consistently been greater than 1.5x10^9/L for over

five years. The patient demonstrated elevated eosinophils (black arrow) in the peripheral blood and BM (Figure 1A). Two distinct populations of ALL cells and eosinophils were observed by flowcytometry analysis, with ALL cells exhibiting classic immunophenotype ($CD19^{+}CD45^{dim}CD10^{+}CD20^{-}CD38^{dim}CD58^{+}$) (Figure 1B). Monitoring of routine blood tests showed similar dynamics of cell counts in ALL and eosinophils following induction therapy (*Online Supplementary Figure S1*). The karyotype revealed 46,XY,t(5;12)(q31;p13),del(11)(p15)[1]/46,XY[23]. RNA-seq was performed on the two populations individually after flow-sorting and *ETV6::ACSL6* was only detected in lymphoblast, while eosinophils did not carry this fusion gene. This indicates that the eosinophil expansion seems to be reactive rather

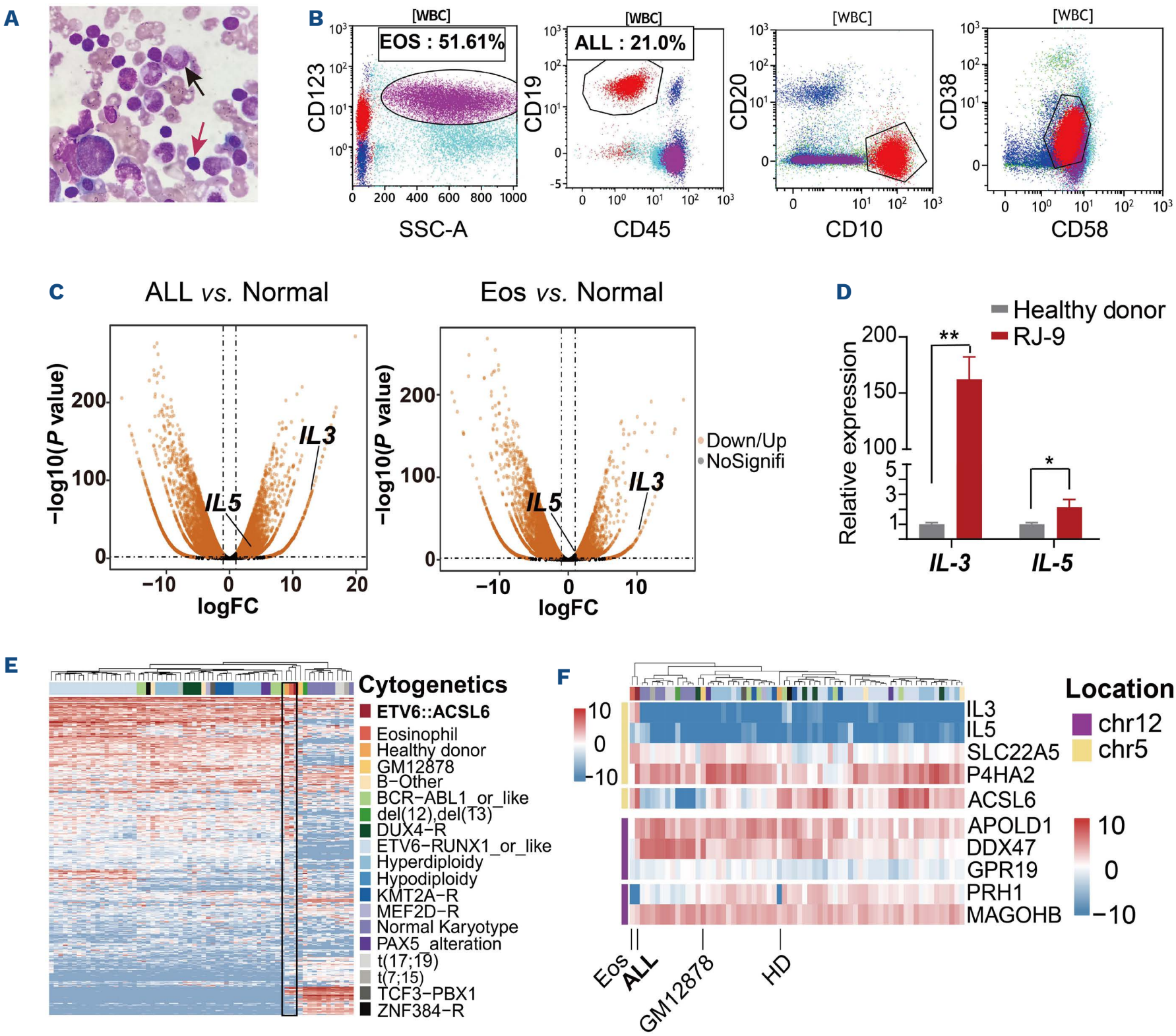

Figure 1. *ETV6::ACSL6* dysregulates the acute lymphoblastic leukemia transcriptome and induces eosinophilia. (A) Representative image of bone marrow (BM) aspiration smear of an *ETV6::ACSL6* patient. Black arrow indicates eosinophils; red arrow indicates acute lymphoblastic leukemia (ALL) cells. (B) Flow cytometry analysis displays eosinophils and ALL cells from BM samples of the *ETV6::ACSL6* patient. Red population refers to ALL cells. (C) Volcano plot showing up-regulated and down-regulated genes in ALL and eosinophils compared to a healthy control. Vertical dashed lines: cutoff of 1.5-fold changes; horizontal dashed lines: cutoff at P=0.05. (D) Fold changes of *IL-3* and *IL-5* expression in an *ETV6::ACSL6* patient compared with a healthy control (N=3). RJ-9: an *ETV6::ACSL6* ALL patient. *P<0.05, **P<0.01. (E and F) Hierarchical clustering of gene expression profiles of *ETV6::ACSL6* ALL in comparison with eosinophils and ALL of various subtypes. (E) Shows all the genes detected. (F) Focused on genes nearby the *ETV6::ACSL6* junction at chr5 and chr12. Chr5 and chr12 are each split into 2 segments: upper portion indicating genes downstream of the breakpoint and lower portion indicating genes upstream of the breakpoint. Each row corresponds to a gene. WBC: white blood cells; Eos: eosinophils; NoSignifi: not significant; HD: healthy donor.

than a clonal proliferation caused by genetic aberrations. Furthermore, analyzing gene expression profiles (GEP) from RNA-seq datasets, we found that *IL-3* and *IL-5* were highly expressed in ALL and eosinophils compared to the normal BM sample (Figure 1C). The result was confirmed by RT-qPCR (Figure 1D). This indicates an intrinsic correlation between inflammatory factors produced by ALL and its accompanying eosinophils with normal karyotype.

Next, comparing GEP of the *ETV6::ACSL6* ALL with previously published RNA-seq datasets of ALL,[22,23] we found that the *ETV6::ACSL6* ALL was clustered with eosinophils, mono-nuclear cells from a healthy BM, and GM12878 cells, but distinct from a well-studied *ETV6* translocation, *ETV6::RUNX1* fusion, suggesting a distinct mechanism of *ETV6::ACSL6* in promoting malignancy transformation (Figure 1E). We further analyzed the top 10 genes that were differentially expressed (also enriched on chr5 and chr12) in the *ETV6::ACSL6* ALL and other ALL subtypes. Interestingly, genes adjacent to the breakpoint of chr5 were significantly up-regulated, including *P4HA2*, *SLC22A5*, *ACSL6*, *IL-3* and *IL-5* (13 Kb, 300 Kb, 40 Kb, 7 Kb and 480 Kb from the breakpoint, respectively), while genes distant from *ETV6* on chr12, such as *PRH1* and *APOLD1* (480 Kb and 1.1 Mb from the breakpoint, respectively), were down-regulated (Figure 1F). This indicates that the perturbations in the ALL transcriptome not only resulted from the potential intragenic SE of *ETV6* promoting genes on chr5, but also from the inactivation of genes on chr12 with the deprivation of *ETV6* regulation.

Multi-omics analysis of *IL-3* activation in *ETV6::ACSL6* acute lymphoblastic leukemia

To further delineate the genetic basis of the fusion gene, we performed long-read sequencing on ALL cells using Oxford Nanopore Technologies (ONT). Both RNA-seq (Figure 2A) and ONT-seq (Figure 2B) demonstrated a breakpoint at the first intron of *ETV6*. RNA-seq identified a fusion of the 1st exon of *ETV6* with the 2nd exon of *ACSL6* in mRNA (Figure 2A, C). However, instead of a DNA break at the *ACSL6* locus, the ONT data revealed a breakpoint at the intergenic region of *ACSL6* and *IL-3* on chr5 (Figure 2B). These data indicate that the fusion of *ETV6* to *ACSL6* revealed by RNA-seq may be due to alternative splicing which skipped the 1st exon of *ACSL* (Figure 2D). We also detected genetic aberrations at various genomic regions, the functions of which are yet to be defined (Figure 2E, *Online Supplementary Table S1*, *S2, Online Supplementary Figure S2*).

The two derivative chromosomes in *ETV6::ACSL6* ALL, i.e., an *ETV6::ACSL6* (EA) strand and an *IL3::ETV6* (IE) strand, are illustrated in *Online Supplementary Figure S3* and verified by RT-PCR in *Online Supplementary Figure S4A*. Analyzing RNA-seq data, we identified a frameshift mutation leading to a premature stop codon (*Online Supplementary Figure S4B*). To confirm the result, we ectopically expressed a full-length EA transcript in Nalm6 (pre-B ALL) cells with a flag peptide at the end of *ACSL6* (*Online Supplementary Figure S4C*). As a control, a wild-type *ETV6*-Flag vector was also transduced, which demonstrated an overexpression of ETV6 and flag proteins (ETV6-OE) (*Online Supplementary Figure S4C*). However, while expression of the EA transcript was verified by PCR (*Online Supplementary Figure S4D*), neither a size shift of the ETV6 protein nor the expression of flag was detected (*Online Supplementary Figure S4E*). In summary, *ETV6::ACSL6* does not give rise to a fusion protein, consistent with previous reports.[6]

Given the scarcity of patient samples, we performed single cell multi-omics sequencing (scNMT-seq) on ALL cells and eosinophils (*Online Supplementary Figure S5A*). UMAP reduction of scRNA data revealed two clusters: a majority ALL cluster expressing cancer-associated genes like *ZFP36L2*, *SF3B1*, and *ARHGDIB*,[24-26] and a smaller cluster comprising eosinophils and some ALL cells (Figure 2F, *Online Supplementary Figure S5B*). Gene set enrichment analysis (GSEA) revealed differentially expressed genes between ALL and eosinophils enriched in hypoxia, unfolded protein response, and DNA repair (p53) pathways, which are reported to be frequently activated in tumors[27] (Figure 2G). Performing scNMT-seq in different subtypes showed that the *IL-3* promoter (orange shading) revealed less enriched methylated-CpG and higher enriched methylated-GpC (accessibility) in the *ETV6::ACSL6* ALL (RJ-9) compared to another ALL (RJ-10) with a normal karyotype (Figure 2H, *Online Supplementary Figure S5C*). The dot plots demonstrated CpG and GpC methylation status in each cell indicating a highly activated *IL-3* in *ETV6::ACSL6* ALL single cells. Moreover, eosinophils exhibited less GpC methylation (accessibility) and higher CpG methylation at the *IL-3* locus than the *ETV6::ACSL6* ALL cells (*Online Supplementary Figure S5D*). Taken together, our data suggest that the *ETV6* translocation altered epigenetic features at genomic regions beyond its fusion partner at chr5.

Furthermore, we extracted enrichments of methylated-CpG and -GpC at promoters for individual cells. Integrating DNA methylation (mCpG), accessibility (GpCm), and RNA transcription through multi-omics factor analysis (MOFA) revealed 3 clusters (*Online Supplementary Figure S5E*), highlighting the epigenetic heterogeneity. mRNA contributed less to cluster identification compared to DNA methylation and chromatin accessibility (5%, 41% and 46% variance in top 5 MOFA factors) (*Online Supplementary Figure S5F*). We then profiled the top 50 differentially methylated regions, identifying two leukemia cells with higher chromatin accessibility and hypomethylation in genes such as *TCF12*, *LIN52* (*Online Supplementary Figure S5G*) that were reported to promote tumor progression.[28,29] Enrichment analysis revealed involvement of metabolic and energetic pathways (*Online Supplementary Figure S5H*), suggesting a connection between metabolic perturbance with epigenetic changes in *ETV6::ACSL6* ALL.

Overall, our data suggest that the *ETV6* translocation in-

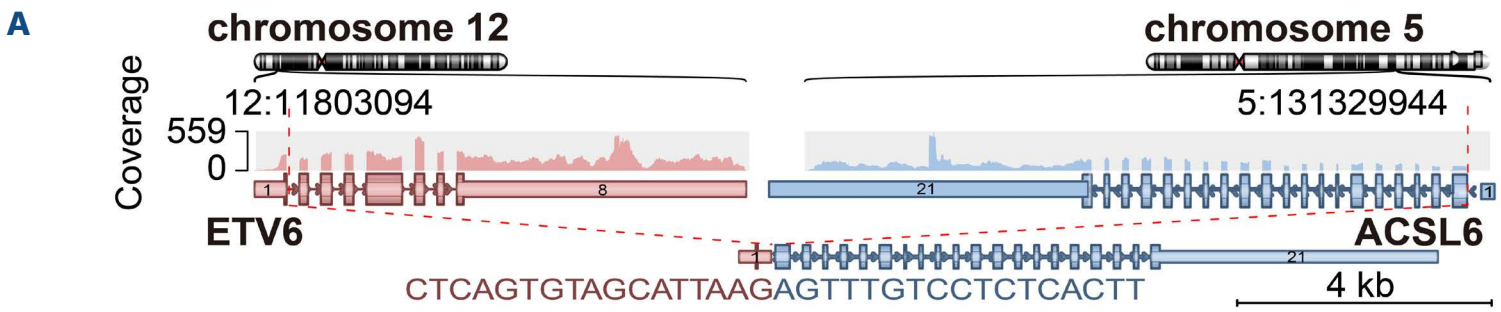

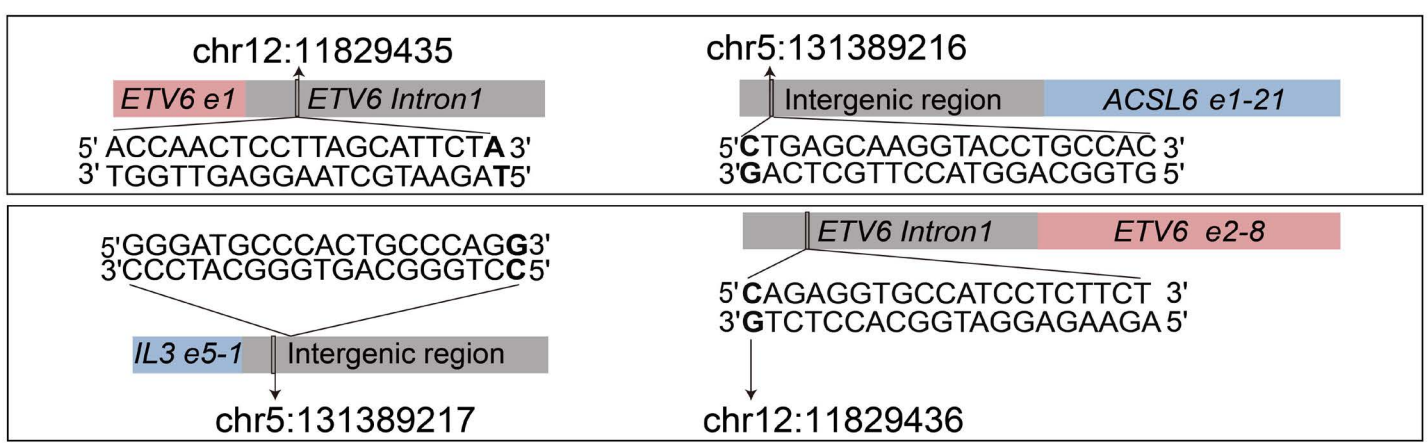

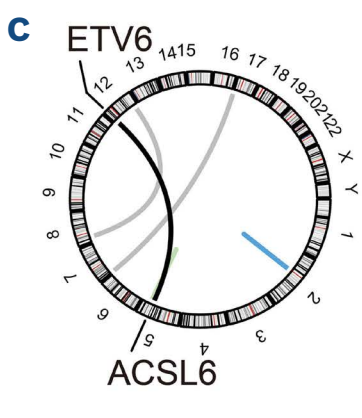

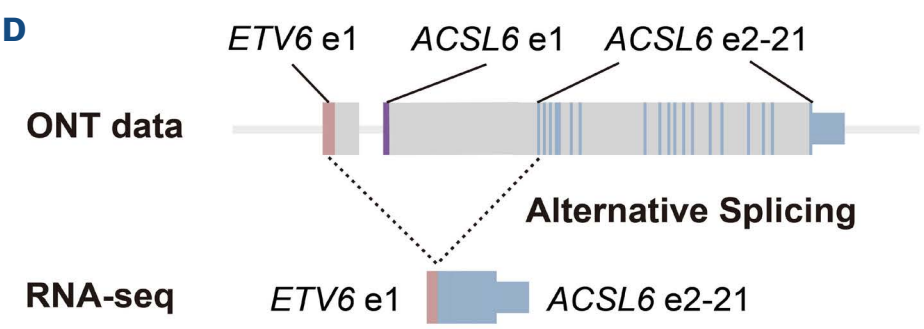

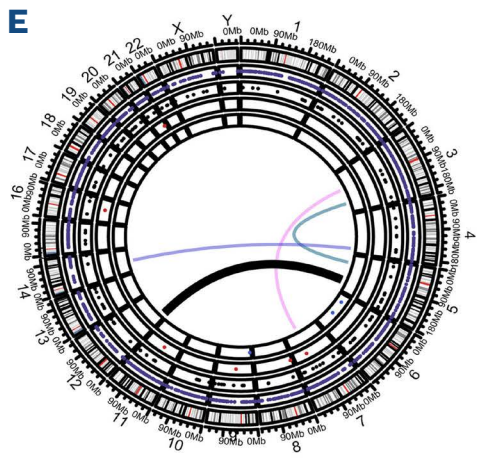

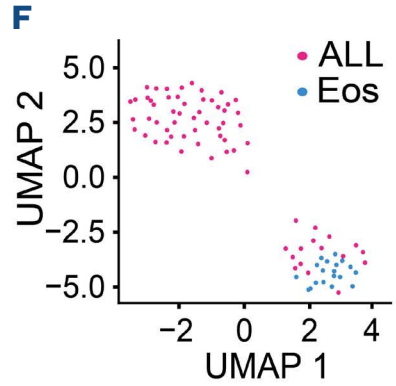

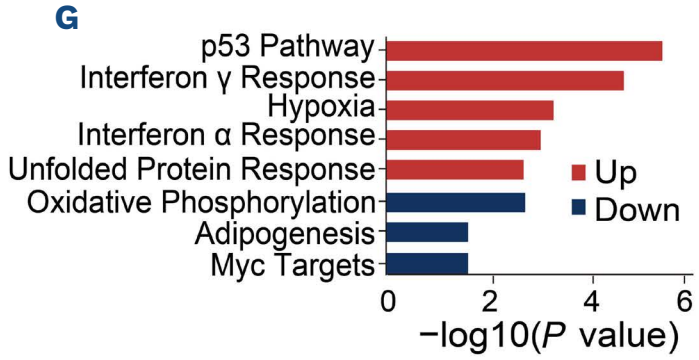

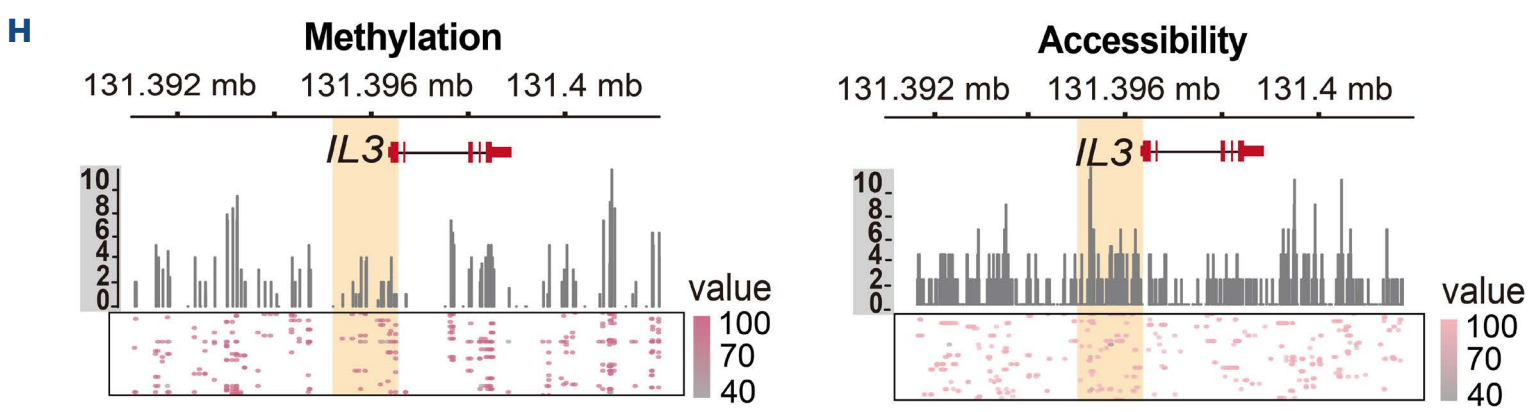

Continued on following page.

Figure 2. Multi-omics analysis of *ETV6::ACSL6* acute lymphoblastic leukemia cells. (A) Mapping of chromosomal breakpoints by RNA-seq revealed a fusion of the first exon of *ETV6* to the second exon of *ACSL6*. (B) DNA sequences nearby the breakpoints on chromosome (chr)12 and chr5 in *ETV6::ACSL6* acute lymphoblastic leukemia (ALL) determined using Oxford Nanopore Technologies (ONT) sequencing. Breakpoints on chr12 and chr5 are indicated by the arrow, and the coordinates are showed. The sequence of 20 base pairs near the breakpoints are also displayed. *IL-3* locus is located at the minus strand of the translocated chr. (C) RNA-seq data showed a fusion of *ETV6* and *ACSL6* genes. Black bar: *ETV6::ACSL6* fusion with highest statistical confidence; gray bars: other fusion events with non-significant statistical confidence; green bar: duplication; blue bar: inversion. (D) Schematic diagram of *ETV6::ACSL6* mRNA splicing. The ONT data and RNA-seq data display the fusion gene at the DNA and RNA levels, respectively. Gray bars: introns; pink bar: exon 1 of *ETV6*; purple bar: exon 1 of *ACSL6*; blue bars: exons 2-21 of *ACSL6*; e1: exon 1; e2-21: exon 2 to 21 of *ACSL6*. (E) Structural variants identified by ONT sequencing. Black bold line: *ETV6::ACSL6* translocation with highest confidence (Variant Allele Frequency=0.9). The other 3 interchromosomal lines are unbalanced translocations. Purple line in the circle: insertion; black line in the circle: deletion; red line in the circle: inversion; blue line in the circle: duplication. (F) UMAP projection analysis of single-cell RNA-seq on ALL and eosinophils. Pink dots: ALL cells; blue dots: eosinophils. (G) Gene Set Enrichment Analysis of differentially expressed genes between ALL and eosinophils. (H) Left: single-cell methylation data at *IL-3* loci; right: single-cell accessibility data at *IL-3* loci. Since cytosines in GpC at open chromatin regions were arbitrarily methylated by adding GpC methyltransferase before bisulfite conversion, the methylated GpC is considered to represent accessible chromatin. Bar plot showing the average level of all cells detected at indicated genomic loci. Each row in the box corresponds to a single cell. Each dot represents the methylation or accessibility level of the corresponding cell (horizontally) at the corresponding genomic position (vertically). RJ-9: an *ETV6::ACSL6* ALL patient.

duced critical epigenetic changes at the gene locus adjacent to the breakpoint on the 2 derivative chromosomes; however, mechanisms causing the abnormal epigenetics remain to be identified.

Chromatin structural variation induced by *ETV6* super-enhancer translocation

Next, we performed SE analysis to explore enhancer activities in diverse cell types. Extracting cell-type specific SE from the SEdb database, encompassing lymphoid, myeloid and other non-hematopoietic cell types, we observed distinctive blood-specific SE, notably the *ETV6* locus (Figure 3A). This suggests that ETV6 serves not only as a crucial transcription factor, but also as an indispensable intragenic hematopoiesis-specific SE in both lymphoid and myeloid cells. In order to validate our findings in *ETV6::ACSL6* ALL, we analyzed H3K4me1 (primed and active enhancers), H3K-27ac (activated enhancers), BRD4 and p300 enrichments at the *ETV6* locus (Figure 3B). Prominent enrichments of H3K27ac and H3K4me1 were identified at the *ETV6* locus, with BRD4, the reader of H3K27ac, also present in this region. The enriched H3K27ac was also observed in B-ALL with normal karyotype (ALL-50 from our previous studies[22]) and cell lines from ENCODE database,[30] suggesting the *ETV6* intragenic region functions as an SE in cis-regulatory machinery. Using the ROSE algorithm,[31] the 200 Kb (chr12:11718965-11902194) region was recognized as a highly-confident SE (Figure 3C). Interestingly, compared to Nalm6, an ALL cell line with *ETV6::PDGFR* fusion, REH with *ETV6::RUNX1* showed decreased H3K27ac enrichment at the *ETV6* locus (Figure 3D), indicating a diminished SE activity in REH. Therefore, the activity of the intragenic SE seems to vary in different *ETV6* fusions.

The *ETV6* locus was split into 2 sections: Pro-SE1 (green rectangle) including the *ETV6* promoter plus a minor SE on the left side; SE2 (blue rectangle) representing the major SE on the right side (Figure 3E). To verify the enhancer activities of 2 sections, we selected a 3Kb region (orange shading) from each section based on transcription factor (TF) binding density and chromatin accessibility (DNase I Hypersensitive Site, DHS) from the ENCODE database and inserted them into a luciferase reporter vector (Figure 3F). While both Pro-SE1- and SE2-inserted vectors revealed significantly enhanced luminescence compared to control, the SE2-inserted vector demonstrated a much more prominent luminescence signal indicating an inherited SE activity (Figure 3G). Motif analysis revealed potential binding sites for TF related to lymphocyte-development / malignancy at the SE, such as Smad3, PAX5 and others (Figure 3H). Overall, the 2 sections of the *ETV6* locus derived from the translocation event maintain enhancer activities, indicating their potential role in regulating ALL genes.

Super-enhancers are clusters of enhancers tightly interacting with multiple adjacent or distal genes.[32] Using high-throughput chromosome conformation capture (Hi-C), we investigated mechanisms of *ETV6*-SE interacting with target genes on a genome-wide scale. *ETV6::ACSL6* ALL displayed a butterfly morphology at the intersection of chr5 and chr12 in the Hi-C heatmap (dotted circles in Figure 4A), whereas GM12878 showed blank, confirming translocation only in RJ-9. Next, using a web-based genome browser,[33] we observed strong interactions between Pro-SE1 and *ACSL6*, enhancing *ACSL6* transcription and H3K27Ac modification in RJ-9 (green dashed lines in Figure 4B). SE2 interacted with multiple downstream genes of *ACSL6*, including strong interactions with *IL-3*, *P4HA2* and a slight interaction with *IL-5* (blue dashed lines in Figure 4B). Consistent with their normally silent state in lymphocytes, GM12878 displayed no active signals for these genes (Figure 4C). Hi-C contact intensities revealed the formation of new topologically associated domains (TAD) spanning the breakpoints with CTCF binding at boundaries, which constrained regulatory activities of Pro-SE1 and SE2, and restricted their target genes (Figure 4D). Neoloop finder identified 69 interchromosomal neoloops on IE and 7 on EA,[34] suggesting uneven activities of Pro-SE1 and SE2 in regulating genes (*Online*

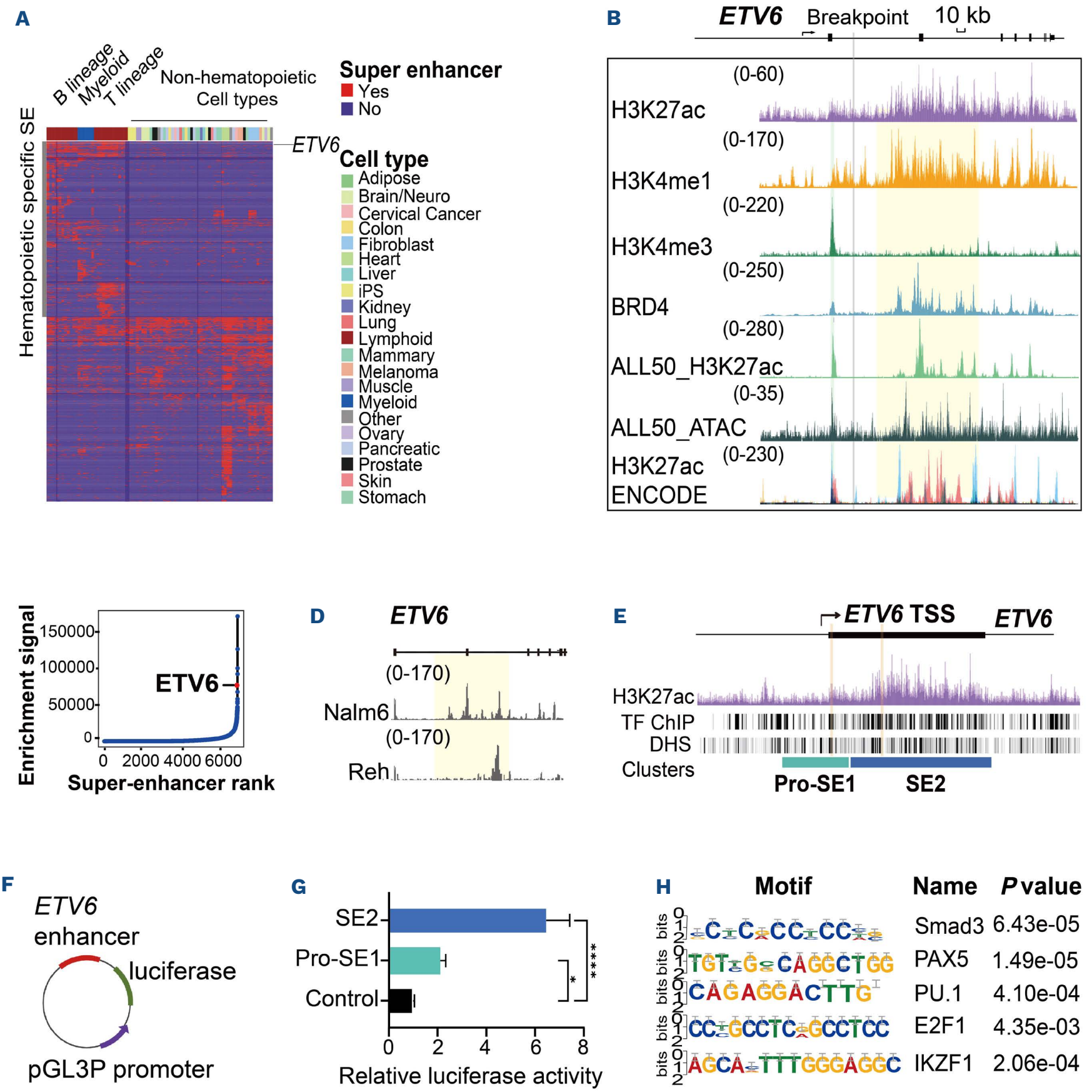

Figure 3. Enhancer hijacking events occur in *ETV6::ACSL6* acute lymphoblastic leukemia. (A) Heatmap of super-enhancer (SE) abundance of 32 hematopoietic and 54 non-hematopoietic cell types from the ENCODE database. Red: detection of SE in the corresponding cell type; purple: not detected. Each column represents a cell type; each row represents an SE coordinate. (B) CUT&Tag profiles for epigenetic marks at the *ETV6* locus in the *ETV6::ACSL6* RJ-9 acute lymphoblastic leukemia (ALL), ALL50 (a normal karyotype ALL patient) and control datasets from ENCODE database. Gray line highlights the breakpoint detected by Oxford Nanopore Technologies (ONT). Green line highlights the promoter of *ETV6*. Yellow bar highlights the main region of *ETV6*-SE. ENCODE: GM12878, H1-hESC, K562. (C) Ranking of SE by analyzing H3K27ac datasets of an *ETV6::ACSL6* patient sample using ROSE algorithm. (D) CUT&Tag profiles of H3K27ac at the *ETV6* locus in Nalm6 and REH cell lines. Nalm6: a pre-B-ALL cell line with *ETV6::PDGFR* translocation; REH: pre-B-ALL cell line with *ETV6::RUNX1* translocation. Yellow shading highlights the *ETV6*-SE identified in the *ETV6::ACSL6* sample. (E) *ETV6* and its promoter region are separated into 2 parts by the breakpoint. Green rectangle: Pro-SE1 (Promoter and left section of *ETV6*); blue rectangle: SE2 (right section of *ETV6*). For the luciferase reporter assay, regions from both Pro-SE1 and SE2 were selected based on TF binding and DNase accessibility from ENCODE, as indicated in orange shading. (F) Schematic depicting the luciferase reporter construct. (G) Luciferase reporter assay. Selected elements in (E) were cloned into a luciferase reporter plasmid pGL3p. The fold inductions were calculated by normalizing to pGL3p control. Statistical significance was calculated using two-tailed *t* tests. Data represent the mean ± Standard Error of Mean of 3 biological replicates. **P*<0.05, *****P*<0.0001. (H) Transcription factor binding site analysis (MEME) of the *ETV6* super-enhancer. The transcription factors were ranked by *P* value, and the top 5 transcription factors are listed.

Supplementary Figure S6). To validate the regulatory effects of the newly formed TAD, we compared gene expression profiles within and outside of the TAD. *ETV6::ACSL6* ALL revealed an upregulation of genes located within the TAD compared to GM12878, whereas genes outside of the TAD did not exhibit significant expression perturbations (Figure 4E). Furthermore, the sustained activity of *ETV6* was also observed in the patient sample with *ETV6::RUNX1*, where the translocated *ETV6* exhibited strong interactions with its partner, *RUNX1*.[35] In *ETV6::ACSL6* ALL, among all genes that are activated due to enhancer hijacking, IL-3 and IL-5 are supposed to promote eosinophilia in patients; furthermore, P4HA2, a proline hydrolase, has been shown to be associated with poor prognosis in diffuse large B-cell

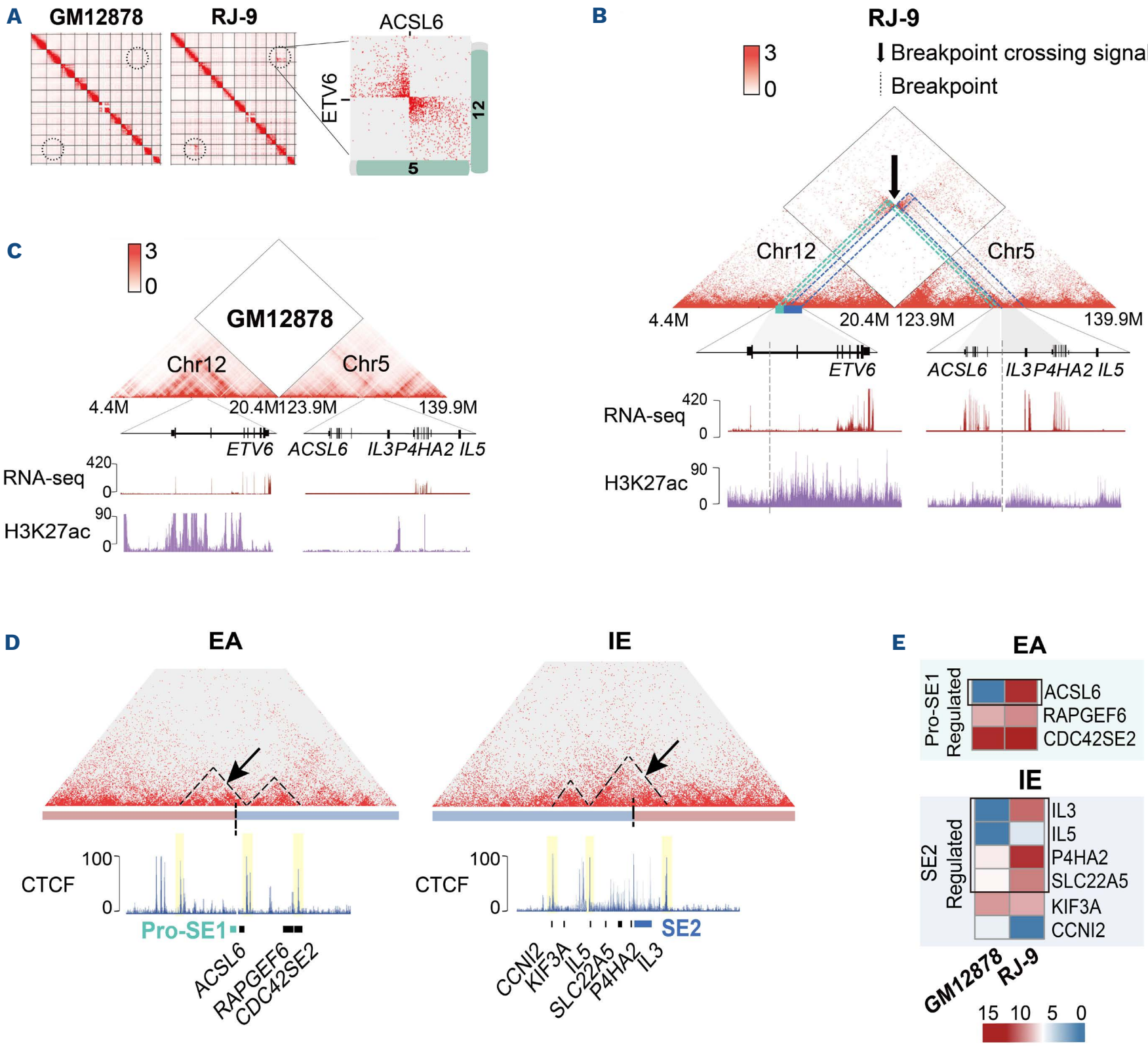

Figure 4. *ETV6::ACSL6* induces changes of chromatin conformation. (A) Visualization of Hi-C data with Juicebox. Dotted circles indicate an interaction between chromosome (chr)5 and chr12. RJ-9: an *ETV6::ACSL6* ALL patient. (B and C) Hi-C data from *ETV6::ACSL6* acute lymphoblastic leukemia (ALL) patient (RJ-9) in comparison with GM12878. Blue dotted lines refer to the interaction between SE2 with target genes, and gray shaded regions indicate the region with stronger interaction. Green dotted lines refer to interactions between Pro-SE1 and target genes. RNA-seq and H3K27ac CUT&Tag coverage are shown below the Hi-C data. Dotted lines indicate the breakpoint on chr12 and chr5. (D) Hi-C maps of rearranged *ETV6::ACSL6* (EA) and *IL3::ETV6* (IE). Black arrows and dashed triangles refer to newly formed topologically associated domains (TAD). Pro-SE1 and SE2 are indicated in green and blue rectangles. Pink bar: chr12; blue bar: chr5. CTCF CUT&Tag coverage is shown below the Hi-C map. Yellow shading highlights CTCF binding boundaries. Vertical dashed lines represent the breakpoint on chr12 and chr5. (E) Gene expression profiles within the newly formed TAD at EA and IE. Black boxes show genes located within the TAD involving Pro-SE1 or SE2.

lymphoma.[36] Studying *P4HA2* expression in our previously reported ALL patients[37] by RNA-seq and qPCR, we found that patients with high expression of *P4HA2* had lower survival rates (*Online Supplementary Figure S7*), indicating that *P4HA2* dysregulation by SE2 may contribute to the poor prognosis of these patients. Overall, our data suggest that hijacking the 2 sections derived from *ETV6*-SE altered 3D genomic organization at new locations, triggering gene transcription exclusively in the *ETV6::ACSL6* ALL and led to its unique clinical characteristics.

Bromodomain and extraterminal domain inhibitors partially reversed gene dysregulation in *ETV6::ACSL6* acute lymphoblastic leukemia

The biological function of SE is often mediated by bromodomain proteins like BRD4 that recognizes highly-enriched acetylated histones at the SE. The bromodomain inhibitor JQ1 has been shown to disrupt enhancer functions, with more pronounced effect on SE.[38] Performing *in vitro* treatment of JQ1 on a patient-derived xenograft (PDX) of the *ETV6::ACSL6* ALL, 1,163 genes were significantly up-regulated and 1,925 down-regulated, including a decrease in *IL-3* (fold change: 0.535887, $P<0.001$) and a mild decrease in *IL-5* (Figure 5A, B). Notably, *MYC* and *BCL2* were also down-regulated in agreement with previous reports on JQ1-induced gene regulation.[39] GSEA revealed inhibited cytokine and Myc-targets pathways (Figure 5C). RT-qPCR confirmed that exposing cells to JQ1 decreased *IL-3* expression in a time- and concentration-dependent manner (Figure 5D). Consistent with this observation, IL-3 concentration in the medium of *ETV6::ACSL6* PDX cell culture decreased after JQ1 treatment; in contrast, *ETV6::RUNX1* cells showed no IL-3 in the medium before and after JQ1 treatment (Figure 5E). As a control, Jurkat cells were pre-stimulated by phytohemagglutinin and phorbol myristate acetate to activate *IL3* expression and followed with JQ1 treatment for 12 hours. RT-qPCR showed a decrease of 50% in *IL3* mRNA after JQ1 treatment, which was significantly lower than the *IL3* decrease in the *ETV6::ACSL6* ALL (*Online Supplementary Figure S8*). Since the *IL3* expression in Jurkat cells without an SE translocation is thought to be regulated by a regular enhancer at *IL3* upstream;[40] this suggests a stronger dependency on BRD4 by SE. Moreover, BRD4 binding was substantially reduced at the whole-genome level and the *ETV6* locus upon JQ1 treatment (Figure 5F-H). Consistent with previous reports,[39] JQ1 altered the genome-wide BRD4 distribution, decreasing at promoters and increasing at intergenic regions (Figure 5 I). Therefore, JQ1 holds promise for dampening gene dysregulation in *ETV6::ACSL6* ALL.

Cytotoxicity of bromodomain and extraterminal domain inhibitor treatment on *ETV6::ACSL6* acute lymphoblastic leukemia *in vitro* and *in vivo*

We then assessed the cytotoxic effects of JQ1 on *ETV6::ACSL6* ALL *in vitro* and *in vivo*. Treatment with JQ1 at concentrations >100nM significantly reduced cell viability *in vitro*, with limited effect on other genetic lesions (Figure 6A, *Online Supplementary Table S3*). JQ1 was then tested in combination with standard-of-care drugs against the *ETV6::ACSL6* ALL. Our data demonstrated synergistic effects of JQ1 with vincristine and doxorubicin, and an additive effect with dexamethasone *in vitro*, with ZIP scores of 24.9, 25.0, and 6.88, respectively (Figure 6B, *Online Supplementary Figure S9A*). Notably, while vincristine or doxorubicin alone achieved 50-70% inhibition of cell viability, the addition of JQ1 (1 μM) substantially decreased the IC_{50} and reduced cell viability to around 10% (Figure 6C, *Online Supplementary Figure S9B*). Furthermore, we

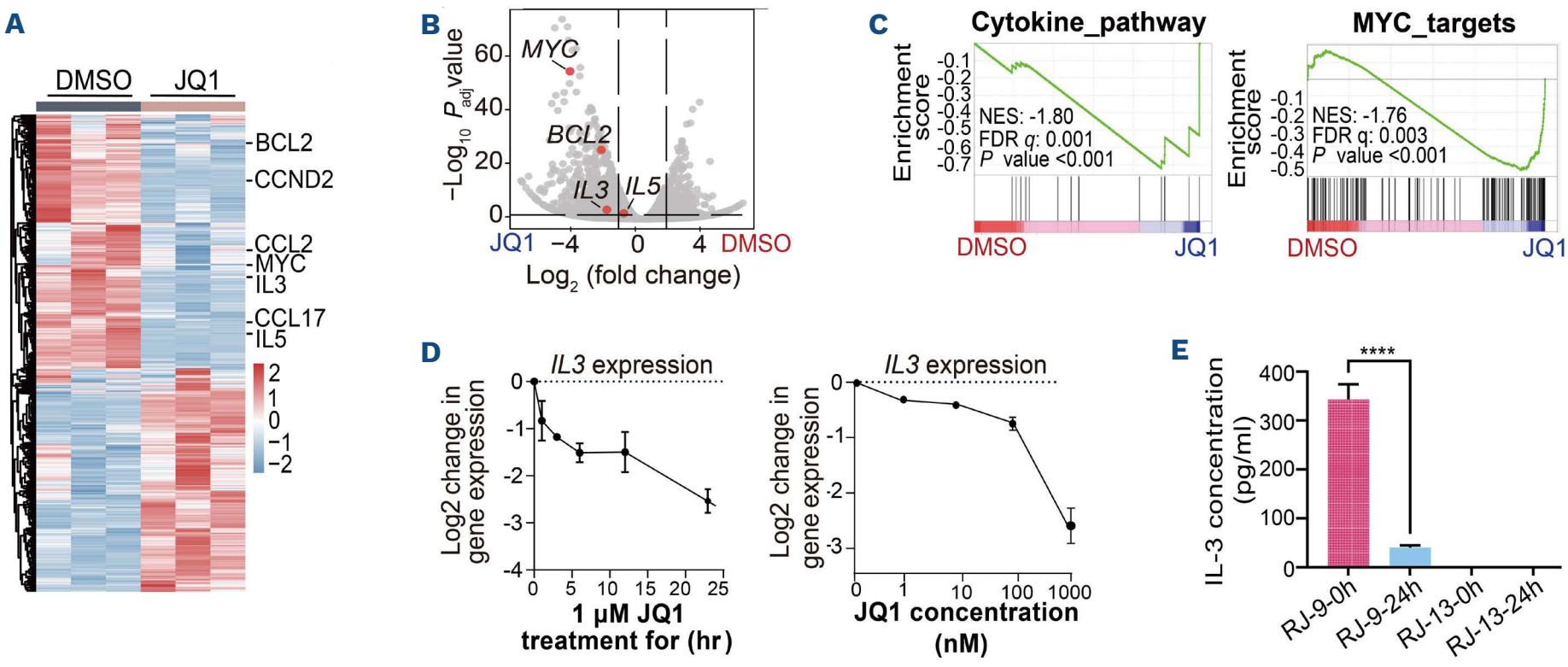

Continued on following page.

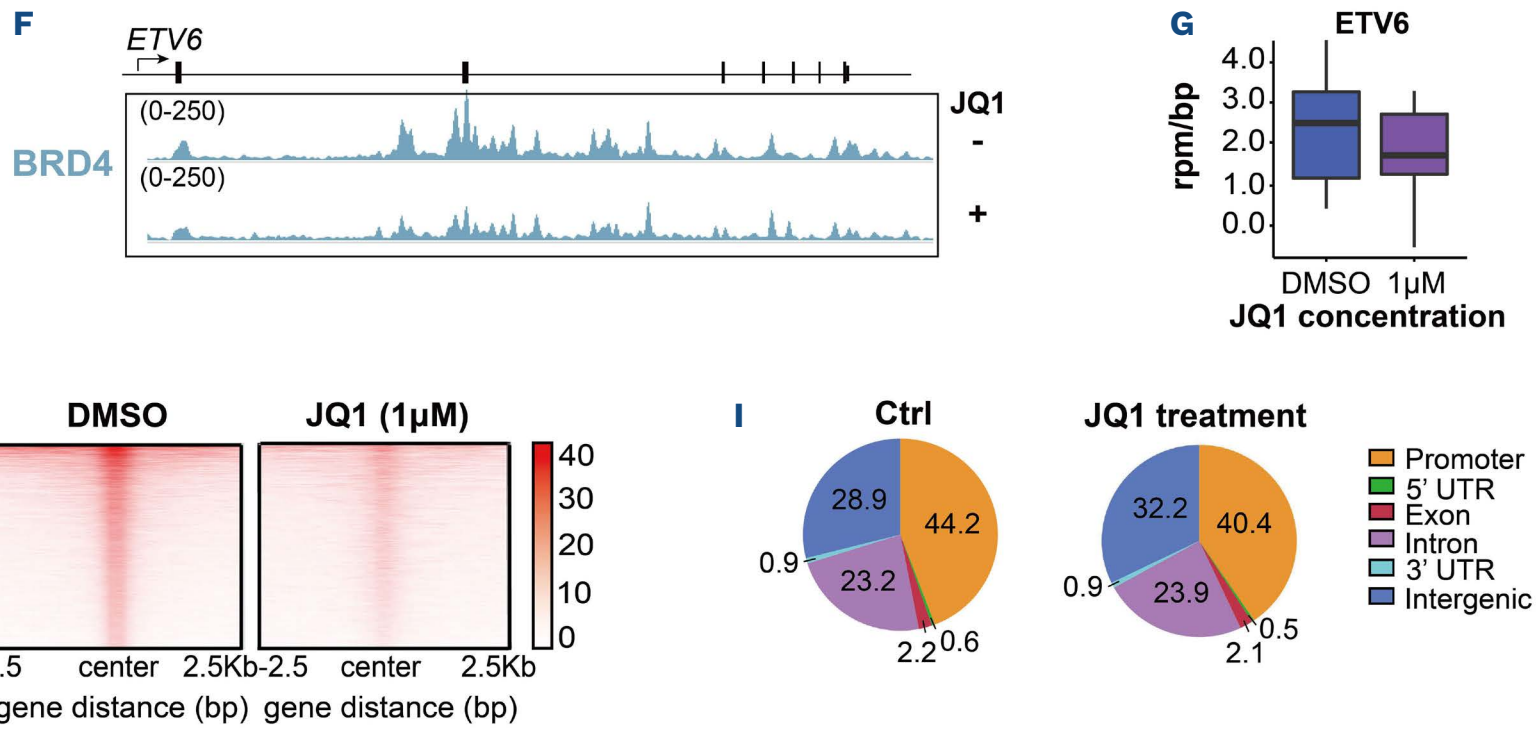

Figure 5. Bromodomain and extraterminal domain inhibitors have the potential to reverse molecular changes caused by the *ETV6* translocation. (A) A heatmap represents the relative expression levels of genes following 1μM JQ1 treatment for 24 hours (hr). Fold change of gene expression under treatment conditions over the control (DMSO) is shown. Exemplary genes are annotated. Each row corresponds to a gene. (B) Volcano plot showing up-regulated (right) or down-regulated (left) following 1μM JQ1 treatment for 24 hr compared with DMSO. (C) Gene Set Enrichment Analysis of DMSO (left) and JQ1 treatment (right). The differentially expressed genes of 2 groups were ranked according to their log10 (*P* value). (D) Downregulation of *IL-3* RNA level by JQ1. *ETV6::ACSL6* acute lymphoblastic leukemia (ALL) cells ($2x10^6$ cells) were treated with JQ1 in a time and concentration dependent manner. (E) IL-3 concentration in the cell culture supernatant following 1μM JQ1 treatment for 24 hr. RJ-9: an *ETV6::ACSL6* ALL patient; RJ-13: an *ETV6::RUNX1* ALL patient. (F) BRD4 occupancy at the *ETV6* gene locus in JQ1 and DMSO treated samples as determined by CUT&Tag. (G) BRD4 enrichment at the *ETV6* locus as determined by CUT&Tag after DMSO (left) or 1μM JQ1 treatment for 24 hr. *y* axis shows BRD4 CUT&Tag signal in units of rpm/bp. (H) Genome-wide BRD4 binding level after 1 μM JQ1 treatment for 24 hr as identified by CUT&Tag. (I) Distribution of genomic elements associated BRD4 peaks following JQ1 treatment. Ctrl: control; BETi: bromodomain and extraterminal domain inhibitors.

tested 5 other commonly-used BET inhibitors: ABBV-744, Birabresib, I-BET151, Mivebresib and PFI-1, and observed their synergistic cytotoxicity with vincristine in treating *ETV6::ACSL6* ALL (Table 1, *Online Supplementary Figure S9C*). Next, *in vivo* treatments were performed as shown in Figure 6D. RT-qPCR revealed a significant decrease in *IL-3* expression following 24-hour *in vivo* treatment of JQ1 and vincristine (Figure 6E). The combination treatment significantly inhibited tumor growth in spleen, BM and peripheral blood at day 28, compared to single-drug treatment with vincristine or JQ1 (Figure 6F, *Online Supplementary Figure S10A, B*). Additionally, we observed that the spleens of the mice in the combination group were dramatically reduced in size after 28 days of treatment compared to those treated with vincristine alone (*Online Supplementary Figure S10C*). One-week post-treatment, the mice treated with vincristine experienced relapse, while the combination group maintained remission for another seven days (Figure 6G). Survival analysis also showed that the combination treatment significantly prolonged the median event-free survival of mice by 9.2 days compared to vincristine alone (Figure 6H). Overall, our data suggest that combining first-line chemotherapy with JQ1 is promising to improve the treatment of *ETV6::ACSL6* B-ALL patients.

Table 1. Combination index of different bromodomain and extraterminal domain inhibitors with vincristine.

Drug 1	Drug 2	Synergy Score
JQ1	Vincristine	24.93
ABBV-744	Vincristine	10.648
OTX015	Vincristine	10.916
I-BET 151	Vincristine	13.846
Mivebresib	Vincristine	13.124
PFI-1	Vincristine	21.124

BET: bromodomain and extraterminal domain.

Discussion

Chromosome translocations often lead to fusion oncogenes, generating fusion proteins interfering with signaling transduction in cancer cells. However, our study confirmed that SV can impact tumor behavior by altering gene expression through enhancer hijacking.[34] In *ETV6::ACSL6* leukemia, a frameshift-induced stop codon prevents protein formation, rendering the fusion protein theory insufficient for explaining eosinophilia. Furthermore, the eosinophils did not carry *ETV6::ACSL6*, indicating eosinophilia as a paraneoplastic

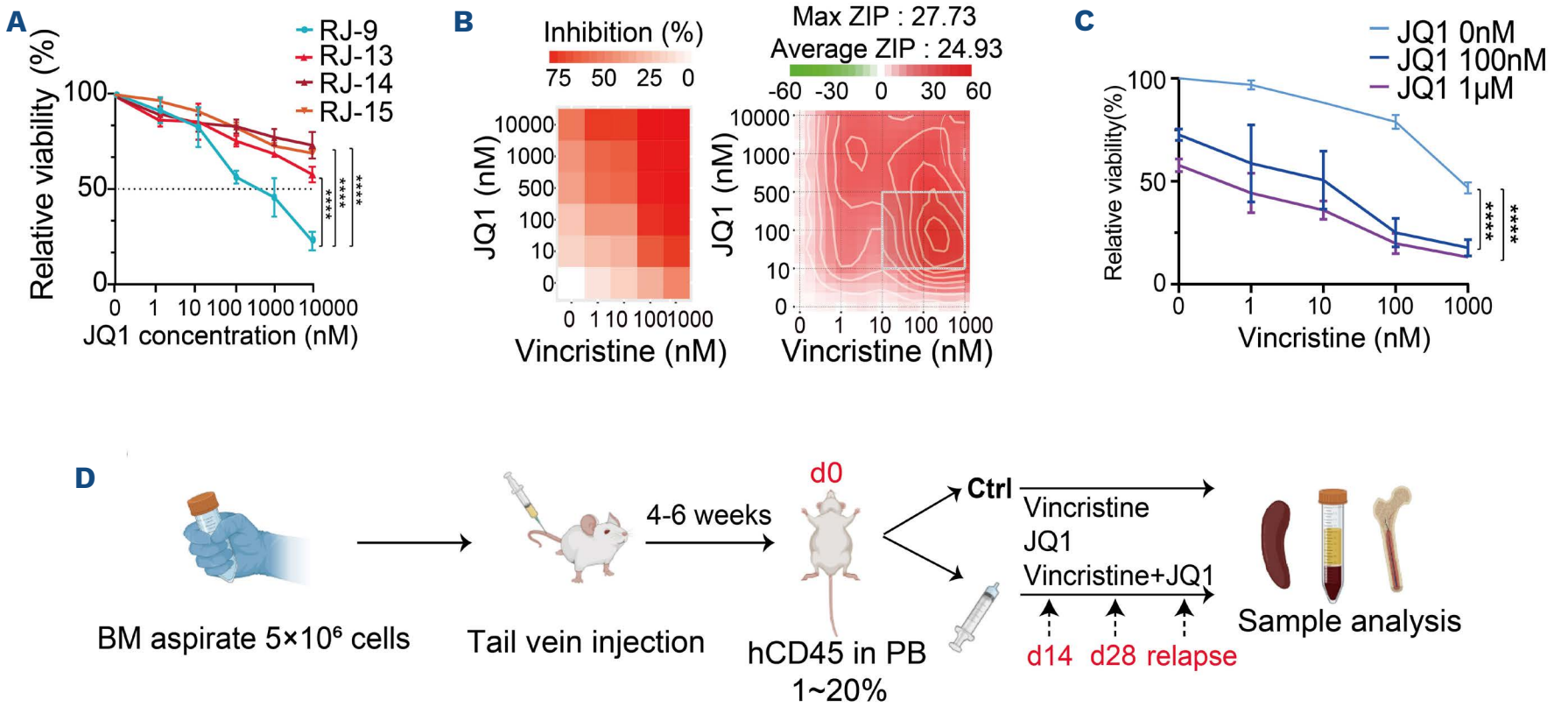

Figure 6. Effects of bromodomain and extraterminal domain inhibitors on *ETV6::ACSL6* acute lymphoblastic leukemia *in vitro* and *in vivo*. (A) Cytotoxicity assay on acute lymphoblastic leukemia (ALL) patient cells with various karyotype. Cells were treated with the indicated concentrations of JQ1. Data represent the mean ± Standard Error of Mean (SEM) of 3 biological replicates. ****P<0.0001. RJ-9: *ETV6::ACSL6*; RJ-13: *ETV6::RUNX1*; RJ-14: *BCR::ABL1*; RJ-15: normal karyotype. (B) Synergistic effect of JQ1 and vincristine in inhibiting cell viability of RJ-9 cells. ZIP: ZIP synergy score.[50] (C) Cytotoxic assay of JQ1 and vincristine at indicated concentrations. ****P<0.0001. (D) Schematic diagram of *in vivo* drug administration. Bone marrow (BM) cells from the *ETV6::ACSL6* patient were harvested and transplanted into NSG mice, which were then treated with JQ1 (50 mg/kg, i.p., five days a week) and vincristine (0.5 mg/kg, i.p., five days a week), separately or in combination for four weeks. Leukemia burden in the peripheral blood (PB) was monitored over time until relapse. After humanely killing the mice, BM and spleens were preserved as mononuclear cells for further use. (E) RNA levels of *IL-3* in different groups after *in vivo* treatment for 24 hours (measured via RT-PCR, N=3). NS: not significant (one-way ANOVA with all samples compared with vehicle control). (F) Assessment of leukemia burden in spleen, BM and PB in an *in vivo* RJ-9 PDX model after 28 days treatment with vincristine (N=4) and combination treatments of JQ1 and vincristine (N=4). Data are represented as a percentage of hCD45⁺ cells for each experiment and expressed as the mean ± SEM; *P<0.05, ***P<0.001 by Mann-Whitney U test. (G) Leukemia burden in the PB over time. (H) Kaplan-Meier curves for event-free survival are shown for vehicle control (N=7), vincristine (N=6), JQ1 (N=5), and combination treatments (N=4) against RJ-9 PDX *in vivo*. Event: % hCD45⁺ cells = 25%. ****P<0.0001 by Gehan-Breslow-Wilcoxon test. d: day; Ctrl: control.

syndrome. Our study identified an SE at the *ETV6* locus and revealed that in *ETV6::ACSL6* ALL, the *ETV6*-SE was split into 2 parts, both exhibiting enhancer activities. This altered chromatin organization in derivative chromosomes, which enhanced the expression of IL-3 and other inflammatory factors, leading to eosinophilia in patients. Our study provides novel insights into cis-regulatory mutation mechanisms associated with this ALL subtype and its clinical complication.

In several *ETV6*-translocation subtypes, fusion proteins were reported to play a dominant role in oncogenesis, most of which function as transcription factors or kinases.[41] For instance, *ETV6::RUNX1*, constituting 13% of B-ALL, was reported to mediate oncogenic activity as a transcription factor.[14] However, mechanisms beyond the trans-regulation by fusion proteins have been poorly studied. In 2021, *ETV6* was reported for the first time to contain an intragenic SE triggering expression of its partner gene *MN1* in *ETV6::MN1* AML.[19] In our study, while Hi-C may not be the optimal technique for quantifying enhancer hijacking events, limiting our ability to accurately assess the interactions between regions, it is still useful for detecting new interactions from the translocated SE and target genes. The translocated *ETV6* regulated not only its fusion partner *ACSL6*, but also distant genes such as *IL-3*, leading to a critical clinical syndrome (eosinophilia) in ALL. Our future work will extend our findings to other *ETV6* fusion partners to gain a comprehensive understanding of the cis-regulatory mechanisms in *ETV6* ALL subtypes.

Our data highlight cis-regulatory mutations controlling the expression of multiple genes, offering potential targets for precision therapy. IL-3, studied for over 30 years, induces proliferation of various cell types, including eosinophils and malignant hematopoietic cells like AML.[42] IL-3 and GM-CSF are crucial in MYC-transduced human hematopoietic cells transitioning to AML, suggesting a crucial role of cytokines in tumorigenesis.[43] Furthermore, *ACSL6* and a distal gene *P4HA2* were also activated by the SE translocation. ACSL6, a long-chain acyl-CoA synthetase, catalyzes long-chain fatty acids.[44] Even though the function of ACSL6 in leukemia is not fully understood, its expression was shown to correlate with the prognosis of AML.[45] Our preliminary studies indicated the association of *P4HA2* with ALL prognosis, which aligns with previous findings in diffuse large B-cell lymphoma.[36] However, the oncogenic role of SE-induced gene overexpression in *ETV6::ACSL6* ALL remains unclear, and this will be addressed in further studies. Nevertheless, according to the 'multi-hit' theory in oncogenesis,[46] SE-induced gene dysregulation may cooperate with other genetic variations driving leukemia transformation and progression.

Eosinophilia accompanying hematologic malignancies has diverse causes, including neoplastic, reactive, or idiopathic. The WHO 2022 classification includes "Myeloid/Lymphoid neoplasms with eosinophilia" (M/LN-Eo) as a separate category, with gene rearrangements of *PDGFRA, PDGFRB* and others.[47] In M/LN-Eo with clonal eosinophilia, gene rearrangements can be detected in eosinophils and other myeloid/lymphoid cell lineages, suggesting pluripotential hematopoietic progenitor cell origin. Conversely, reactive eosinophilia often results from tumors secreting cytokines, such as IL-3. Examples of such tumors include Hodgkin lymphoma[48] and our case of *ETV6::ACSL6* ALL. Therefore, it is critical to determine different treatment strategies, considering varied causal mechanisms of eosinophilia in hematologic malignancies. Besides glucocorticoids, the conventional treatment for eosinophilia, other targeted options are being explored. Clonal eosinophilia bearing fusion genes may benefit from tyrosine kinase inhibitors,[47] but the choice is limited for reactive eosinophilia, which often causes severe symptoms and hinders primary disease treatment. In *ETV6::ACSL6* ALL, with eosinophilia linked to elevated IL-3, drugs targeting IL-3 pathways are considered. Furthermore, BRD4 inhibitors have achieved promising anti-tumor effects in various preclinical studies.[49] Since the translocated SE conferring IL-3 elevation was highly enriched with BRD4, its inhibition significantly dampened the SE-induced gene expression, and synergized with first-line chemotherapy drugs in treating *ETV6::ACSL6* ALL *in vitro* and *in vivo*. This demonstrates the potential of new therapeutic approaches for *ETV6::ACSL6* ALL.

Overall, our study reports for the first time that *ETV6* translocation led to chromatin structural variations in ALL patients, which resulted in dysregulation of inflammatory factors conferring eosinophilia in ALL. This highlighted the crucial role of enhancer hijacking in oncogenesis and particularly its clinical complications, and provided insights into improving treatment strategies for this ALL subtype with unfavorable prognosis.

Disclosures

The authors have no conflicts of interest to disclose. Any opinions, findings, conclusions or recommendations expressed in this publication do not reflect the views of The Government of the Hong Kong SAR, the Innovation and Technology Commission or the Vetting Committee of the Mainland-Hong Kong Joint Funding Scheme of the Innovation and Technology Fund.

Contributions

DJ, JM and JW designed the study. WX performed experiments and analyzed the data. FT performed bioinformatics analysis. WX, DJ and JM interpreted the data and wrote the manuscript. XT, GS and MW assisted in performing experiments. JM, JW, YL, LF and XW interpreted the clinical data. JWHW and EY contributed to bioinformatics analysis. MB, CZ, RBL and JWHW contributed to the data interpretation and revision of the manuscript.

Acknowledgments

The authors thank Prof. Heather Lee (University of Newcastle, Australia) for assistance in establishing the single-cell technique. The authors acknowledge the ENCODE Consortium for generating DNaseI HS datasets and TF ChIP-seq datasets.

Funding

This research was funded by grants from the National Key R&D Program of China (2022YFE0200100), the Innovation Program of Shanghai Science and Technology Committee (23141903000, 21430711800), the National Natural Science Foundation of China (NSFC 82070144, 82270155, 82070227, 32271165, 82270187), the Mainland-Hong Kong Joint Funding Scheme supported by the Innovation and Technology Commission, the Government of Hong Kong SAR, China (MHP/054/21), the Ideas Grant funding of the National Health and Medical Research Council of Australia (APP1181666), and the Mobility Programme of the Joint Committee of the Sino-German Center for Research Promotion by the NSFC and the Deutsche Forschungsgemeinschaft (M-0337). RBL is supported by a fellowship from The National Health and Medical Research Council of Australia (NHMRC Fellowship APP1157871).

Data-sharing statement

The raw sequencing data from this study have been deposited in the Genome Sequence Archive in National Genomics Data Center, Beijing Institute of Genomics (BIG), Chinese Academy of Sciences, under the accession number: HRA004277, that are publicly accessible at https://ngdc.cncb.ac.cn/gsa. We also host a UCSC browser session for easy access and viewing of genome-wide mapping at: http://genome-asia.ucsc.edu/s/xuwenqian/RJ9_data. All other relevant data that support the conclusions of the study are available from the authors on request. Please contact jdh12262@rjh.com.cn.

References

1. Mitelman F, Johansson B, Mertens F. The impact of translocations and gene fusions on cancer causation. Nat Rev Cancer. 2007; 7(4):233-245.
2. Li JF, Dai YT, Lilljebjörn H, et al. Transcriptional landscape of B cell precursor acute lymphoblastic leukemia based on an international study of 1,223 cases. Proc Natl Acad Sci U S A. 2018;115(50):E11711-E11720.
3. Chen B, Jiang L, Zhong ML, et al. Identification of fusion genes and characterization of transcriptome features in T-cell acute lymphoblastic leukemia. Proc Natl Acad Sci U S A. 2018;115(2):373-378.
4. Rasighaemi P, Ward AC. ETV6 and ETV7: siblings in hematopoiesis and its disruption in disease. Crit Rev Oncol Hematol. 2017;116(2):106-115.
5. Zaliova M, Moorman AV, Cazzaniga G, et al. Characterization of leukemias with ETV6-ABL1 fusion. Haematologica. 2016;101(9):1082-1093.
6. Zhou MH, Gao L, Jing Y, et al. Detection of ETV6 gene rearrangements in adult acute lymphoblastic leukemia. Ann Hematol. 2012;91(8):1235-1243.
7. Bain BJ, Ahmad S. Should myeloid and lymphoid neoplasms with PCM1-JAK2 and other rearrangements of JAK2 be recognized as specific entities? Br J Haematol. 2014;166(6):809-817.
8. Zimmermannova O, Doktorova E, Stuchly J, et al. An activating mutation of GNB1 is associated with resistance to tyrosine kinase inhibitors in ETV6-ABL1-positive leukemia. Oncogene. 2017;36(43):5985-5994.
9. Su Z, Liu X, Hu W, et al. Myeloid neoplasm with ETV6::ACSl6 fusion: landscape of molecular and clinical features. Hematology. 2022;27(1):1010-1018.
10. Cools J, Mentens N, Odero MD, et al. Evidence for position effects as a variant ETV6-mediated leukemogenic mechanism in myeloid leukemias with a t(4;12)(q11-q12;p13) or t(5;12)(q31;p13). Blood. 2002;99(5):1776-1784.
11. Esnault S, Kelly EA. Essential mechanisms of differential activation of eosinophils by IL-3 compared to GM-CSF and IL-5. Crit Rev Immunol. 2016;36(5):429-444.
12. Patel B, Kang Y, Cui K, et al. Aberrant TAL1 activation is mediated by an interchromosomal interaction in human T-cell acute lymphoblastic leukemia. Leukemia. 2014;28(2):349-361.
13. Huang Y, Mouttet B, Warnatz HJ, et al. The leukemogenic TCF3-HLF complex rewires enhancers driving cellular identity and self-renewal conferring EP300 vulnerability. Cancer Cell. 2019;36(6):630-644.
14. Polak R, Bierings MB, van der Leije CS, et al. Autophagy inhibition as a potential future targeted therapy for ETV6-RUNX1-driven B-cell precursor acute lymphoblastic leukemia. Haematologica. 2019;104(4):738-748.
15. Adnan-Awad S, Kim D, Hohtari H, et al. Characterization of p190-Bcr-Abl chronic myeloid leukemia reveals specific signaling pathways and therapeutic targets. Leukemia. 2021;35(7):1964-1975.
16. Yagasaki F, Jinnai I, Yoshida S, et al. Fusion of TEL/ETV6 to a novel ACS2 in myelodysplastic syndrome and acute myelogenous leukemia with t(5;12)(q31;p13). Genes Chromosomes Cancer. 1999;26(3):192-202.
17. López C, Burkhardt B, Chan JKC, et al. Burkitt lymphoma. Nat Rev Dis Primers. 2022;8(1):78.
18. Rawat VP, Cusan M, Deshpande A, et al. Ectopic expression of the homeobox gene Cdx2 is the transforming event in a mouse model of t(12;13)(p13;q12) acute myeloid leukemia. Proc Natl Acad Sci U S A. 2004;101(3):817-822.
19. Riedel SS, Lu C, Xie HM, et al. Intrinsically disordered Meningioma-1 stabilizes the BAF complex to cause AML. Mol Cell. 2021;81(11):2332-2348.
20. Argelaguet R, Clark SJ, Mohammed H, et al. Multi-omics profiling of mouse gastrulation at single-cell resolution. Nature. 2019;576(7787):487-491.
21. Clark SJ, Smallwood SA, Lee HJ, Krueger F, Reik W, Kelsey G. Genome-wide base-resolution mapping of DNA methylation in single cells using single-cell bisulfite sequencing (scBS-seq). Nat Protoc. 2017;12(3):534-547.
22. Jing D, Huang Y, Liu X, et al. Lymphocyte-specific chromatin

accessibility pre-determines glucocorticoid resistance in acute lymphoblastic leukemia. Cancer Cell. 2018;34(6):906-921.
23. Yu CH, Wu G, Chang CC, et al. Sequential approach to improve the molecular classification of childhood acute lymphoblastic leukemia. J Mol Diagn. 2022;24(11):1195-1206.
24. Fang F, Lu J, Sang X, et al. Super-enhancer profiling identifies novel critical and targetable cancer survival gene LYL1 in pediatric acute myeloid leukemia. J Exp Clin Cancer Res. 2022;41(1):225.
25. Han C, Khodadadi-Jamayran A, Lorch AH, et al. SF3B1 homeostasis is critical for survival and therapeutic response in T cell leukemia. Sci Adv. 2022;8(3):eabj8357.
26. Zhu J, Tian Z, Li Y, et al. ATG7 promotes bladder cancer invasion via autophagy-mediated increased ARHGDIB mRNA stability. Adv Sci (Weinh). 2021;8(22):e2104365.
27. Zhang Y, Wang S, Zhang J, et al. Elucidating minimal residual disease of paediatric B-cell acute lymphoblastic leukaemia by single-cell analysis. Nat Cell Biol. 2022;24(2):242-252.
28. Zhang Y, Yu R, Li Q, et al. SNHG1/miR-556-5p/TCF12 feedback loop enhances the tumorigenesis of meningioma through Wnt signaling pathway. J Cell Biochem. 2020;121(2):1880-1889.
29. Luo Z, Li X, Zhao Z, Yang X, Xiao S, Zhou Y. MicroRNA-146a affects the chemotherapeutic sensitivity and prognosis of advanced gastric cancer through the regulation of LIN52. Oncol Lett. 2017;13(3):1386-1392.
30. The ENCODE Project Consortium. An integrated encyclopedia of DNA elements in the human genome. Nature. 2012;489(7414):57-74.
31. Whyte WA, Orlando DA, Hnisz D, et al. Master transcription factors and mediator establish super-enhancers at key cell identity genes. Cell. 2013;153(2):307-319.
32. Hnisz D, Abraham BJ, Lee TI, et al. Super-enhancers in the control of cell identity and disease. Cell. 2013;155(4):934-947.
33. Wang Y, Song F, Zhang B, et al. The 3D Genome Browser: a web-based browser for visualizing 3D genome organization and long-range chromatin interactions. Genome Biol. 2018;19(1):151.
34. Wang X, Xu J, Zhang B, et al. Genome-wide detection of enhancer-hijacking events from chromatin interaction data in rearranged genomes. Nat Methods. 2021;18(6):661-668.
35. Mallard C, Johnston MJ, Bobyn A, et al. Hi-C detects genomic structural variants in peripheral blood of pediatric leukemia patients. Cold Spring Harb Mol Case Stud. 2022;8(1):a006157.
36. Jiang W, Zhou X, Li Z, et al. Prolyl 4-hydroxylase 2 promotes B-cell lymphoma progression via hydroxylation of Carabin. Blood. 2018;131(12):1325-1336.
37. Gao M, Wang J, Rousseaux S, et al. Metabolically controlled histone H4K5 acylation/acetylation ratio drives BRD4 genomic distribution. Cell Rep. 2021;36(4):109460.
38. Filippakopoulos P, Qi J, Picaud S, et al. Selective inhibition of BET bromodomains. Nature. 2010;468(7327):1067-1073.
39. Lovén J, Hoke HA, Lin CY, et al. Selective inhibition of tumor oncogenes by disruption of super-enhancers. Cell. 2013;153(2):320-334.
40. Baxter EW, Mirabella F, Bowers SR, et al. The inducible tissue-specific expression of the human IL-3/GM-CSF locus is controlled by a complex array of developmentally regulated enhancers. J Immunol. 2012;189(9):4459-4469.
41. De Braekeleer E, Douet-Guilbert N, Morel F, Le Bris MJ, Basinko A, De Braekeleer M. ETV6 fusion genes in hematological malignancies: a review. Leuk Res. 2012;36(8):945-961.
42. Aldoss I, Clark M, Song JY, Pullarkat V. Targeting the alpha subunit of IL-3 receptor (CD123) in patients with acute leukemia. Hum Vaccin Immunother. 2020;16(10):2341-2348.
43. Bulaeva E, Pellacani D, Nakamichi N, et al. MYC-induced human acute myeloid leukemia requires a continuing IL-3/GM-CSF costimulus. Blood. 2020;136(24):2764-2773.
44. Rossi Sebastiano M, Konstantinidou G. Targeting long chain Acyl-CoA synthetases for cancer therapy. Int J Mol Sci. 2019;20(15):3624.
45. Chen WC, Wang CY, Hung YH, Weng TY, Yen MC, Lai MD. Systematic analysis of gene expression alterations and clinical outcomes for long-chain acyl-coenzyme A synthetase family in cancer. PLoS One. 2016;11(5):e0155660.
46. Gilliland DG, Tallman MS. Focus on acute leukemias. Cancer Cell. 2002;1(5):417-420.
47. Shomali W, Gotlib J. World Health Organization-defined eosinophilic disorders: 2022 update on diagnosis, risk stratification, and management. Am J Hematol. 2022;97(1):129-148.
48. Francischetti IMB, Alejo JC, Sivanandham R, et al. Neutrophil and eosinophil extracellular traps in Hodgkin lymphoma. Hemasphere. 2021;5(9):e633.
49. Guo J, Zheng Q, Peng Y. BET proteins: biological functions and therapeutic interventions. Pharmacol Ther. 2023;243:108354.
50. Ianevski A, Giri AK, Aittokallio T. SynergyFinder 2.0: visual analytics of multi-drug combination synergies. Nucleic Acids Res. 2020;48(W1):W488-W493.